# REPORT DOCUMENTATION PAGE

*Form Approved*
*OMB No. 0704-0188*



| **1. REPORT DATE** *(DD-MM-YYYY)* | **2. REPORT TYPE** | **3. DATES COVERED** *(From - To)* |
|---|---|---|
| July 2014 | Technical Paper | May 2014- July 2014 |

**4. TITLE AND SUBTITLE**
A Computational Study of Transverse Combustion Instability Mechanisms

**5a. CONTRACT NUMBER**

**5b. GRANT NUMBER**

**5c. PROGRAM ELEMENT NUMBER**

**6. AUTHOR(S)**
Shipley, K., Anderson, W., Harvazinski, M. and Sankaran, V.

**5d. PROJECT NUMBER**

**5e. TASK NUMBER**

**5f. WORK UNIT NUMBER**
Q12J

**7. PERFORMING ORGANIZATION NAME(S) AND ADDRESS(ES)**

Air Force Research Laboratory (AFMC)
AFRL/RQR
5 Pollux Drive
Edwards AFB CA 93524-7048

**8. PERFORMING ORGANIZATION REPORT NO.**

**9. SPONSORING / MONITORING AGENCY NAME(S) AND ADDRESS(ES)**
Air Force Research Laboratory (AFMC)
AFRL/RQR
5 Pollux Drive
Edwards AFB CA 93524-7048

**10. SPONSOR/MONITOR'S ACRONYM(S)**

**11. SPONSOR/MONITOR'S REPORT NUMBER(S)**
**AFRL-RQ-ED-TP-2014-203**

**12. DISTRIBUTION / AVAILABILITY STATEMENT**
Distribution A: Approved for public release; distribution unlimited

**13. SUPPLEMENTARY NOTES**
Technical paper presented at the 50th AIAA Joint Propulsion Conference, Cleveland, OH, 07/28/2014. PA#14357

**14. ABSTRACT**
Computational fluid dynamics simulations are used to study spontaneous combustion instabilities in a rectangular chamber that contains seven coaxial injector elements. The simulation predicts self-excited transverse oscillations that have variable amplitudes, similar to what is seen in a companion experiment. Several processes are identified in the simulation that may promote the rise of instability by increased heat release during a local compression, including the interaction between vortices shed from adjacent injectors and interactions between flames and the combustor walls.

**15. SUBJECT TERMS**

| **16. SECURITY CLASSIFICATION OF:** | | | **17. LIMITATION OF ABSTRACT** | **18. NUMBER OF PAGES** | **19a. NAME OF RESPONSIBLE PERSON** |
|---|---|---|---|---|---|
| | | | | | V. Sankaran |
| **a. REPORT** | **b. ABSTRACT** | **c. THIS PAGE** | SAR | 16 | **19b. TELEPHONE NO** *(include area code)* |
| **Unclassified** | **Unclassified** | **Unclassified** | | | 661-275-5534 |

# A Computational Study of Transverse Combustion Instability Mechanisms

Kevin J. Shipley[1], William E. Anderson[2]
*Purdue University, West Lafayette, IN, 47906*

Matthew E. Harvazinski[3], and Venkateswaran Sankaran[4]
*Air Force Research Laboratory, Edwards AFB, CA, 93524*

**Computational fluid dynamics simulations are used to study spontaneous combustion instabilities in a rectangular chamber that contains seven coaxial injector elements. The simulation predicts self-excited transverse oscillations that have variable amplitudes, similar to what is seen in a companion experiment. Several processes are identified in the simulation that may promote the rise of instability by increased heat release during a local compression, including the interaction between vortices shed from adjacent injectors and interactions between flames and the combustor walls.**

## I. Introduction

COMBUSTION instability is one of the main technical risks for rocket engine development programs. To date no methodology exists to reliably predict combustion instability *a priori* in a full-scale engine. Recent advancements in computational fluid dynamics (CFD) are however helping to promote a further understanding about the initiation and sustenance of combustion instability. The focus of the present research is on applying CFD to high-frequency, transverse combustion instabilities in a subscale model rocket combustor to assess the capability to predict self-excited instabilities in a multi-element configuration, and to investigate the interactions between injector element flows, unsteady heat release and resonant gas dynamics in the combustor.

High-frequency combustion instability arises when the heat release from combustion couples with the acoustic modes of a chamber. While potentially present in all combustion devices, liquid rocket engines are particularly susceptible due to extreme energy densities and low levels of acoustic damping. During naturally unsteady combustion, acoustic waves are produced that interact with the reacting flowfield. The acoustics serve as a feedback mechanism, influencing combustion processes, which may in turn amplify or attenuate the acoustic waves. This coupling is dependent on many factors including the method of propellant injection, flowfield structure, combustor geometry, and their influence on one another. High-frequency acoustic instabilities can occur in longitudinal, transverse, spinning, and mixed modes. A longitudinal instability is characterized by waves that travel along the main combustor axis. These waves reflect back and forth between the injector face and converging-diverging nozzle to form a standing longitudinal mode. In a transverse instability, waves instead propagate perpendicularly to the axial flow, reflecting off the chamber side-walls. The transverse modes are generally considered to be more destructive than longitudinal modes because the increased acoustic velocity near the injector face increases local mixing, heat release, and hence the face heat flux.

Interactions between the unsteady flowfield and flame can have a direct impact on the presence and amplitude of combustion instability. Vortex interactions have been theorized to be one source capable of driving combustion instability. Smith and Zukowski[1] demonstrated that vortices containing unreacted fuel and oxidizer can couple with the acoustics field to serve as a source to regularly feed energy to sustain combustion instability. In non-premixed systems, the vortices entrain incoming fuel and are convected downstream, igniting at a later time. The vortices have

[1] Graduate Research Assistant, School of Aeronautics and Astronautics and Member AIAA.
[2] Professor, School of Aeronautics and Astronautics and Associate Fellow AIAA.
[3] Scientist, Rocket Propulsion Division and Member AIAA.
[4] Senior Scientist, Rocket Propulsion Division and Senior Member AIAA.

been shown to break down when they impinge on another vortex or surface boundary, causing an increase in mixing and flame surface area.[2,3] The cycle continues as more velocity perturbations leading to vortex formation are induced by the strengthened acoustic field. Other sources of heat release perturbations were investigated by Ducruix et al.[3] who found that energy could be fed into the acoustic field through flame interactions with a wall, unsteady strain rates, and fluctuating equivalence ratios.

Whereas direct measurement of these processes in experiments is difficult, improving capabilities in reacting CFD simulations can help lead to a better understanding of combustion instability behavior. The key has been the application of large eddy simulations (LES) or hybrid forms of LES that allow the resolution of large-scale eddies that play an important role in the reacting flow dynamics. Studies have shown that LES can model the coupling between the heat release and the acoustic modes.[4-11] Many of these studies have also been instrumental in shedding light on the key underlying mechanisms that lead to the occurrence and sustenance of combustion instabilities.

Simulations to date have primarily focused on simple geometries, many of which are single-injector configurations. Both two-dimensional axisymmetric simulations and full three dimensional simulations have been used. Simulations of multi-injector configurations have taken place to a lesser degree. The research in this paper builds upon previous work using a multi-injector approach to study injector response to transverse.[12] Shipley et al.[12] showed that the response of an injector to transverse oscillations could be represented by applying artificial driving conditions at the wall boundaries. While the results were fairly successful in matching experimental injector response, this approach does not allow for the study of the source of instability, or for the interactions between the injector elements.

Instability behavior is largely determined by the injector element type. In this study, an oxidizer-centered coaxial element similar to what is used in the main chamber of oxidizer-rich staged-combustion rocket engines is used. Several recent CFD simulations have provided insight to the combustion dynamics behavior in single-element rocket combustors that demonstrate self-excited instabilities. Smith et al.[13, 14] performed 2D-axisymmetic simulations to study longitudinal instabilities. It was shown that the instability mechanism was related to vorticity pulsing in the oxidizer post and vortex impingement on the chamber wall. Three-dimensional simulations of the same single-injector combustor were better able to capture the higher order harmonic modes with limit cycle amplitudes that approached the experimental data.[10,15] Harvazinski et al.[16] further identified three influential processes of the instability mechanism. The first process was the timing of pressure pulses between the combustor and oxidizer post. At high amplitudes, the longitudinal waves traveling upstream into the oxidizer post interrupted the fuel flow and allowed unburnt fuel to accumulate near the dump plane. When the reflected wave in the element and/or the combustor impacted the partially premixed oxidizer and fuel, rapid burning occurred which served to sustain the compression wave. Other important processes included increased mixing due to baroclinic torque which produced vorticity and the presence of a tribrachial flame as a strong source for unsteady heat release. The existence of the tribrachial flame in this combustor was earlier identified by Garby et al.[11] Harvazinski et al.[16] also noted the complexity of the triple flame dynamics, moving throughout the combustor, with periodic extinction and re-ignition.

Limitations still exist in these models however, both with respect to computational capability and understanding the degree of modeling fidelity required for any specific set of physics. Not all of the physical processes can be simulated or modeled accurately. Comparisons with experiments are limited due to available measurement techniques, and even methods for comparison are not well-developed due to the complexity of the problem. Computational run-time is another issue, since the large unsteady calculations may take several months to complete. Currently it is still too expensive to routinely simulate a full-scale engine with CFD, although capabilities are continually growing and combustion dynamics in a full-annular gas turbine burner has been simulated recently.[17] There is also ongoing work to extend subscale results to full-scale engines by using data from experiments and validated CFD simulations to develop combustion response functions for engineering-level design analysis models.[18]

The approach described here uses a subscale injector with seven elements. The transverse mode of the rectangular chamber is on the order of 2 kHz, which is similar to transverse mode frequencies in full-scale rocket combustors. The main objective of this study is to investigate whether a full-geometry computational model of the transverse instability combustor (TIC) can match combustion instability behavior measured in a companion experiment.[19] A key aspect is the ability of the model to capture the self-excited coupling of the combustion and the acoustics leading to growth and limit cycle of the pressure oscillations. Further objectives are to investigate the response of the injector elements to transverse oscillations and to identify physical processes that can influence the combustion instability phenomena.

The outline of this paper is as follows. First, a description of the hybrid RANS/LES code used to simulate the experiment is given, followed by a description of the model geometry and boundary conditions. Then simulation results are presented. First, a description of the flowfield is presented along with an identification of some of the

influential processes, which include vortex interactions in the chamber flowfield and their interaction with the acoustics. Following this, the instability behavior of the combustor is investigated, taking a look at different vorticity interactions during different stages of the instability process.

## II. Computational Setup

### A. Solver

The General Equation and Mesh Solver (GEMS) is the CFD code that is used in the present study. GEMS is a second-order implicit finite-volume code,[20-23] which solves the Navier-Stokes equations, comprised of the continuity, momentum, energy, turbulence, and coupled species equations. A source term is introduced in the species conservation equations for species production and consumption. A dual-time iterative procedure is used to eliminate linearization and approximate factorization errors. Turbulence is modeled using a hybrid RANS/LES model.[24,25] In the model, large eddies are resolved in the region where the grid resolution is sufficient. In areas where the grid resolution is insufficient, like the near-wall region, turbulence effects are modeled using a two-equation $k$-$\omega$ model.[26,27] A laminar flame-rate model is used and all species are modeled using an ideal gas equation of state. Thermodynamic and transport properties are evaluated through polynomial fit data.[28]

### B. Geometry and Grid Generation

The geometry is modeled after the companion TIC experiment similar to that presented by Morgan et al.[19] The geometry and mesh are shown in Figure 1. The model includes all seven injector elements. Decomposed hydrogen peroxide is used for the oxidizer and the fuel is gaseous methane. A choke plate is modeled in the center injector to choke the oxidizer flow. In the companion experiment, oxidizer flow is choked in the outer six injectors with converging–diverging nozzles at the inlets. These are not modeled in the simulation, but instead constant mass flow inlets are employed. The simplification does not account for shock wave effects from the nozzles on any acoustic waves travelling upstream in the oxidizer tubes. Fuel is injected in an annulus about the oxidizer core and flows coaxially into the main chamber. Fuel flows in the outer four injectors and center injector. Similar to the experiment, the injectors on either side of the center element flow oxidizer only so that the flame emission observed through a window near the center injector can be directly tracked to just the fuel injected by the center injector. The main chamber is rectangular and converges to a choked throat. The mesh was developed from a reduced geometry model[12] and further modified. The mesh contains 11.7 million hexahedral cells with $y^+$ values of unity adjacent to the combustion chamber and nozzle walls.

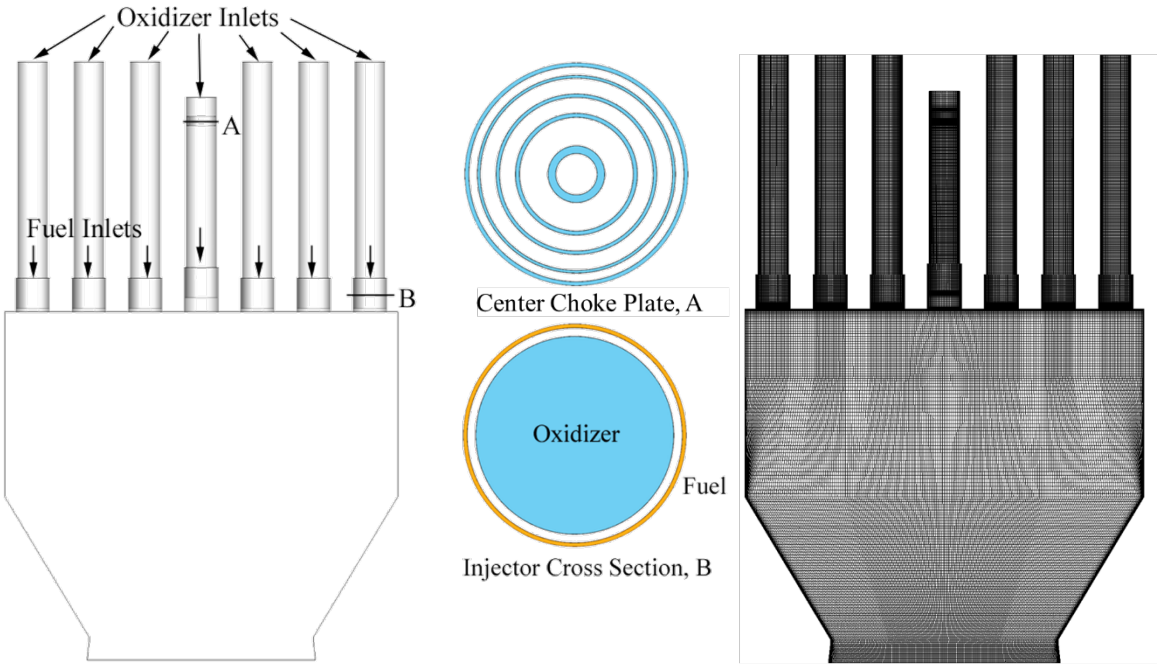


**Figure 1: Model geometry (left) with cross section slices (center) showing the oxidizer flow (in blue) through the choke plate (A) and oxidizer and coaxial fuel flow through the injector (B). The computational mesh is shown to the right with 11.7 million hexahedral cells.**

## C. Boundary Conditions and Initial Conditions

The boundary conditions applied in the simulation include 14 mass flow inlets, which permit the reflection of compression waves. Seven of the fourteen are the oxidizer inlets, which are circular and are located upstream as shown in Figure 1. The other seven are the fuel inlets, which have an annular shape and are located near the base of the injectors. The specific mass flow conditions specified at the boundary inlets are shown in Table 1.

**Table 1: Mass flow inlet boundary conditions, mass flows are per injector.**

| Inlet | Mass flow, kg/s | Temperature, K | Species Concentration |
|---|---|---|---|
| Oxidizer | 0.195 | 1029 | 42% $O_2$, 58% $H_2O$ |
| Center injector fuel | 0.025 | 298 | 100% $CH_4$ |
| Driving injector fuel | 0.033 | 298 | 100% $CH_4$ |

Downstream of the combustor throat the backpressure is set to ambient pressure with a six-degree half-angle nozzle expansion to ensure that the flow is choked at the throat. All walls are no-slip and adiabatic. The initial condition in the chamber is adjusted to closely resemble the conditions in the experiment. The geometry is initially filled with decomposed hydrogen peroxide (42% $O_2$ and 58% $H_2O$) at 1500K in the combustion chamber and 1029K everywhere else. The initially warm temperature in the chamber ensures that the methane fuel will ignite upon mixing with the oxidizer. It is noted that attempts to run the simulations with an initial temperature of 1029K did not result in ignition.

## D. Reaction Kinetics

Combustion is modeled using a single-step global methane reaction, which incorporates the four species: $CH_4$, $O_2$, $H_2O$, and $CO_2$. Using a global reaction reduces the number of coupled species equations that must be solved while

maintaining a pressure dependent reaction rate. The reaction is shown in Eq. 1 and the species production is determined from the parameters presented in Table 2. The parameters are based on experimental data to match laminar flame speeds.[29]

$$CH_4 + 2O_2 \rightarrow CO_2 + 2H_2O$$

Eq. 1

**Table 2: Single step methane reaction parameters.**

| Parameter | Equation 1 |
|---|---|
| A , $\frac{1}{k^{n_S}}\left(\frac{gmol}{cm^3}\right)^{1-a-b}$ | 6.7E12 |
| $E_{A,}$ kcal/gmol | 48.4 |
| a | 0.2 |
| b | 1.3 |

## III. Results and Discussion

### A. Flowfield Overview

The chamber is initially filled with decomposed hydrogen peroxide modeled as 42% $O_2$ and 58% $H_2O$. At the onset of the simulation, diaphragms are broken at the oxidizer and fuel inlets and a constant mass flow of methane enters the domain through the outer four fuel annuli and center annulus. A constant mass flow of 42% $O_2$ and 58% $H_2O$ enters through the oxidizer inlets. The nozzle throat becomes choked almost immediately. As the methane gas reaches the 1500K gas filling the chamber, it reacts and produces a strong ignition spike that sends pressure waves reflecting against the combustor walls. As the reflecting pressure waves die down from the ignition spike, reacting fuel and oxidizer continue to fill the chamber as shown in Figure 2. Periodic vortices begin to shed from the injector lips, entrapping fuel and promoting mixing. As the fuel and oxidizer burn in the chamber, products exit through the choked nozzle.

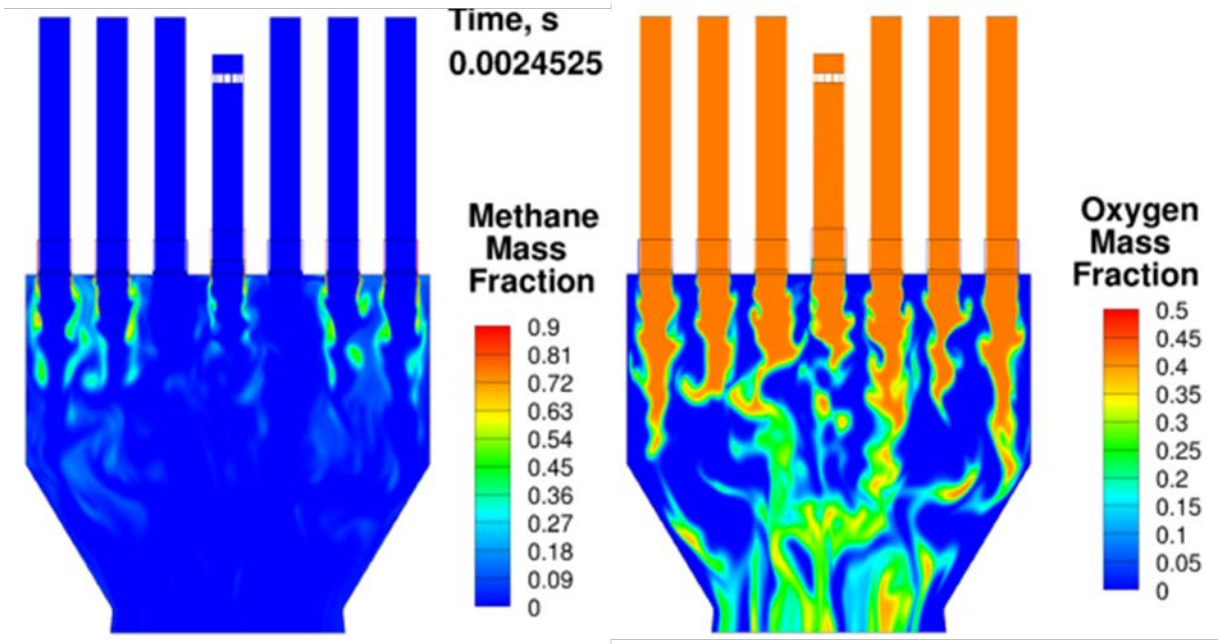


**Figure 2: Methane fuel injection (left) and oxidizer injection (right).**

A transverse mode with a frequency of 2 kHz quickly develops in the rectangular chamber. The traversing pressure wave is depicted in Figure 3 for half of a cycle at about 9 ms into the simulation. The first frame shows the time at which the left wall pressure is at its highest value. Compression waves are sent upstream in the three left injectors. In frames two and three, the wave can be seen reaching the converging wall on the right side of the combustor. As the wave fills in the upstream portion of the chamber compression waves are sent upstream into the injectors on the right side. Lastly, in the fourth frame the wave has fully traversed the chamber and a pressure maximum occurs on the right side of the chamber. As the transverse wave moves back and forth across the chamber, and sends waves up into the injector elements, the unsteady velocity field in the element induces the formation of periodic vortices that are shed from the injector lips. The coherent bundles of partially mixed fuel and oxidizer that are transported downstream by the vortices are susceptible to rapid reaction if they are impacted by a compression wave or hot wall.

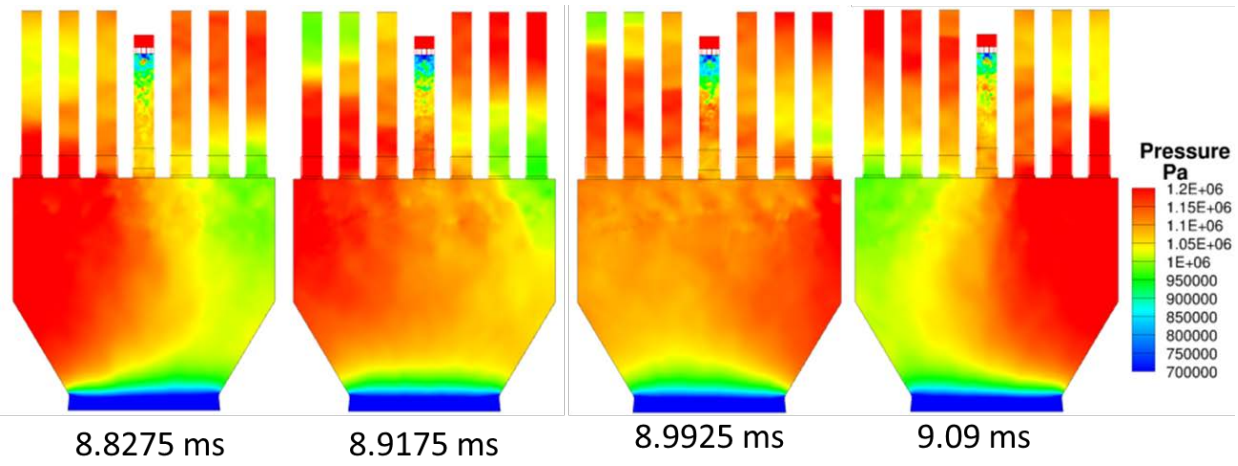


**Figure 3: A transverse wave travels from left to right across the simulation covering a half instability cycle.**

The transverse mode depicted in Figure 3 is generated without artificial forcing. The mechanism which is theorized to cause self-excitation is related to the vortices that are shed from the side injectors that impinge on the side-wall at the first acoustic mode frequency. The timing between the combustor pressure oscillations and the vortex formation is such that the vortices impinge coincidentally with a pressure maximum, sending an additional energy pulse into the acoustic field. The overall process can be described sequentially as follows. Transverse waves in the combustor are transmitted into the injector tubes, and set up resonant fluid motion. The resonant fluid motion, specifically accelerates velocity in the tube flow, resulting in vortices shed off the injector lip. The vortices entrain fuel; as the vortex travels downstream, fuel and oxidizer continue to mix. The vortex either impinges on the wall, or it is impacted by the incoming compression wave that was reflected off the opposite wall, both of which cause rapid mixing and reaction.

Several regions of interest are observed in the simulation that may support this theoretical mechanism. Regions where vortices are observed interacting between adjacent injector elements and interacting with the side-wall are shown in Figure 4. All the images represent slices through the center of the chamber at the same instance in time. Image 1 shows the vorticity field. A high amount of vorticity is generated at the exit of the choke plate of the center injector. Vortices are shed at the lips of the outer six injectors as the transverse wave moves back and forth across the chamber and the compression waves are reflected within the oxidizer tubes. The vortex formation may be influenced by several different effects including the baroclinic torque that is caused by the pressure and density gradients from the reflected compression waves. The vortices are also under the influence of the transverse motion of the wave in the chamber, which can cause vortex stretching through velocity gradients.

The region outlined in orange shows where vortices interact between injector elements. Image 2 shows the methane fuel trapped in vortices shed from the lip. Between injectors 6 and 7 (box b) methane is rolled up into vortices that may mix together and burn with oxidizer from either injector core. Between injectors 5 and 6, only one fuel vortex is seen near the injector face as only oxidizer flows through injector 5. A slice of the corresponding heat release contour is shown in image 3. As the vortices mix with the oxidizer they produce a small amount of heat release. Vortices also impinge when they are pushed together by the transverse wave.

The region outlined in purple shows a zone downstream of the injector face where vortices impinge against the side-wall. When this happens a pulse in the heat release can be produced because the vortex impingement enhances the mixing between the entrained fuel and the oxidizer flow. Image 4 shows two zones that highlight where fuel is entrained in vortices. It is the fuel in the first zone (box a) that is impinging against the wall. The fuel in the second zone (box b) had previously impinged against the wall and has continued to move downstream. It is the fuel in box b that is actually burning as shown by the heat release in image 6. This appears commonly throughout the simulation where a fuel entrained vortex will impinge against the wall; continue to mix with the oxidizer stream and burn more at a later instant in time.

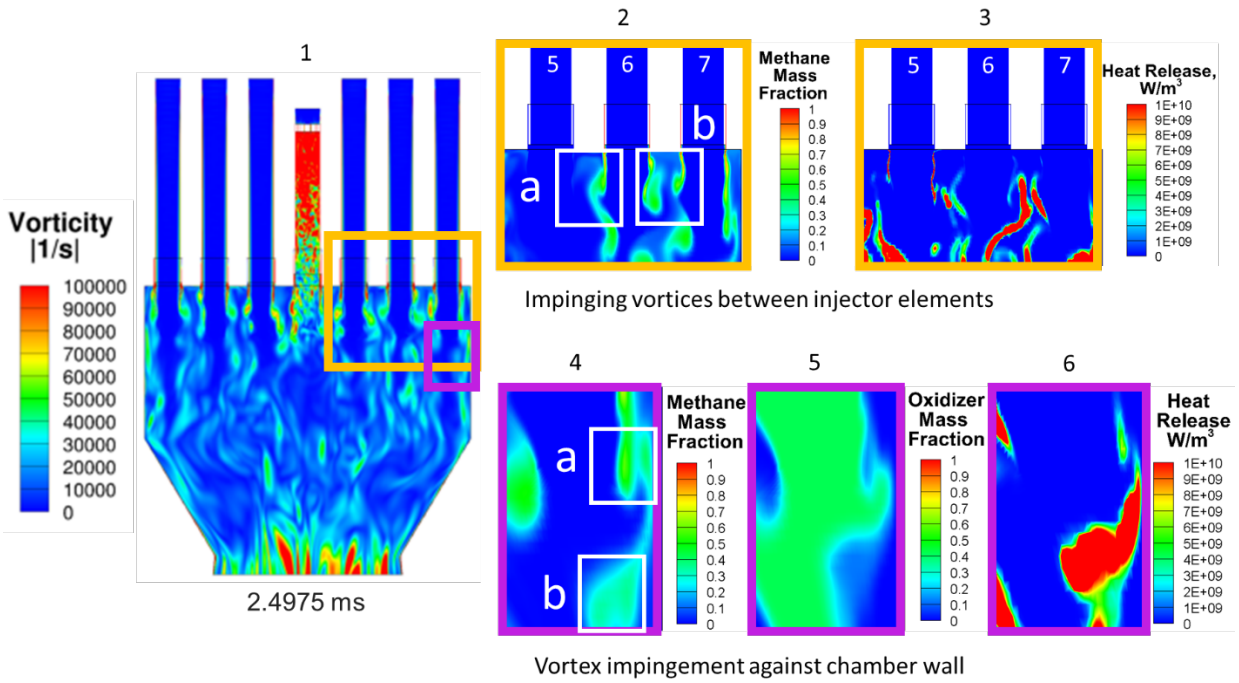


**Figure 4: Several vortex impingement locations are observed in the simulation. Vortices are observed impinging between adjacent injector elements (region in orange) and along the chamber side walls (region in purple).**

## B. Instability startup

The simulation produces a range of instability amplitudes as shown in Figure 5. After the ignition spike, low amplitude instability is observed with pressure fluctuations ranging from 10-20% of the mean chamber pressure (0.97 MPa). The pressure measurement is taken at the left wall, which is the location of an antinode for the first acoustic mode. The corresponding frequencies in the signal are shown below by applying a short-time Fourier transform over four different regions. The primary frequency during the low amplitude instability stage is centered at the first acoustic mode around 2 kHz and lasts until 7.5 ms. After the period of low amplitude instability, the combustor switches to a strong growth phase to high amplitude instability, with pressure oscillations approaching 70% of the mean chamber pressure. A change in frequency of the signal is also observed during this stage. Not only is a strong concentration seen at the first acoustic mode of 2 kHz but also at the higher harmonics, which are integer multiples of the first mode. The higher modes become evident as the amplitude grows and the waves steepen.

During startup, low frequency heat release oscillations appear as shown in the spatially averaged heat release signal presented in Figure 6. The heat release is spatially averaged over the chamber volume (as indicated in Figure 6) and fluctuates at a 1 kHz frequency, which is half the frequency of the first acoustic mode. The first peak is due to the ignition spike and leads to reflecting pressure waves along the wall boundaries. A wave-front is sent upstream into the injector posts, which reflects back downstream and generates vortices. After the ignition spike, fuel and oxidizer continue to fill in the main chamber, mixing along the way and producing more heat release while the 1 kHz oscillation dies down. Around 3 ms, the fuel and oxidizer have filled the combustor. As the fuel and oxidizer fill the chamber, pressure fluctuations arise throughout, appearing chaotic. Out of these apparently random pressure fluctuations, a strong pressure spike develops at the right side of the chamber around 2.4 ms, which coincides with the time that the flame from the right-most injector reaches the converging section of the chamber. The oxygen mass fraction and the pressure contours at this instant in time is shown in Figure 7.

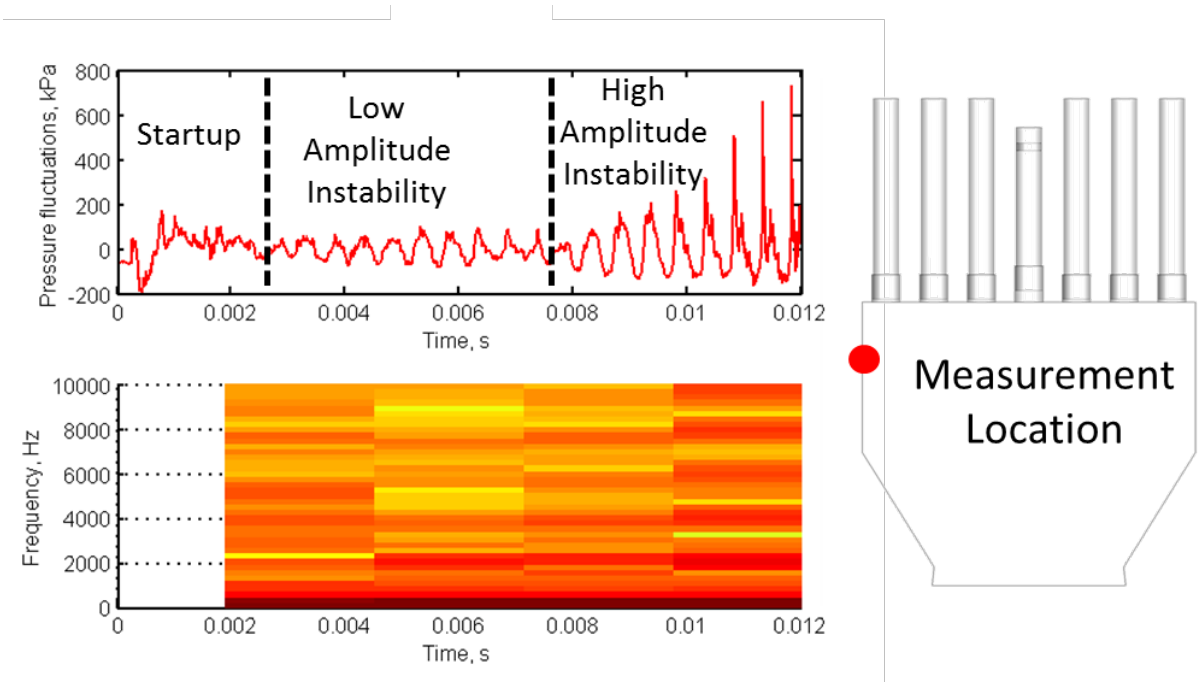


**Figure 5: The instability amplitude in the chamber changes over time, revealing stages of low amplitude instability and high amplitude instability. The pressure fluctuation measurement is taken at the left wall and the corresponding frequency of the signal is plotted underneath.**

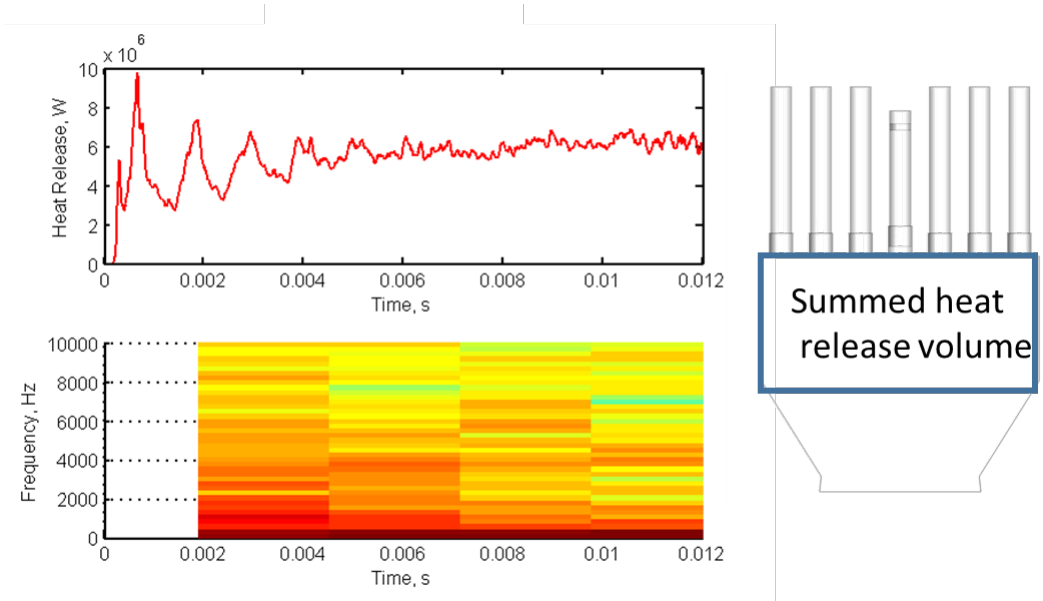


**Figure 6: Spatially averaged heat release is plotted through time. The volume averaged over is shown at the right and the corresponding frequency in the signal is plotted in the bottom image with an initial frequency concentration of 1 kHz.**

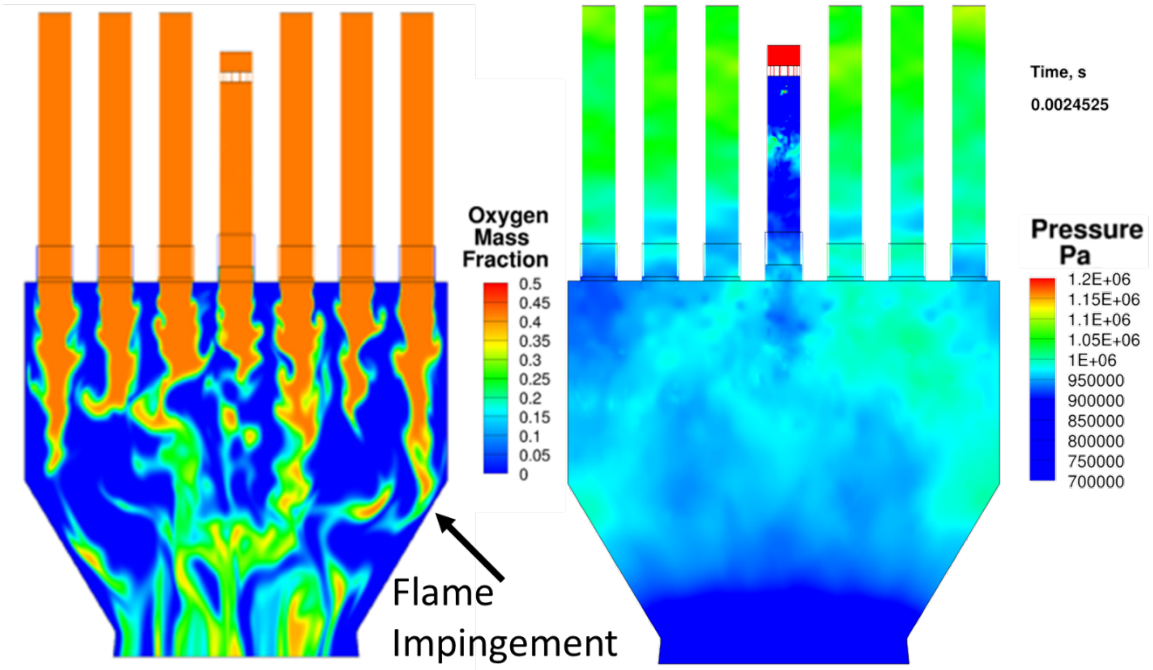


**Figure 7: The transverse mode first appears as a strong pressure concentration develops in the right side of the chamber (right) while the flame from the right side of the injector impinges against the converging chamber section shown by the oxygen mass fraction (left).**

As the cycle continues pressure fluctuations appear in the left side of the chamber and the left injector flame impinges against the chamber converging section. Transverse motion develops in the fluid flow and the side injector flames continue to impinge at the nozzle converging sections, alternating back and forth and generating additional pressure pulses. The relationship between the flame and wall boundary layer appears to be important with the flame impingement providing a source for initial pressure fluctuations in the chamber. This mechanism is an extension to the previously described vortex impingement mechanism, which focused on the impingement of vortices on the chamber side-walls close to the injectors.

## C. Low Amplitude Instability

The period of low amplitude instability arises when the transverse motion of the fluid becomes sustained. Several processes are observed which may be responsible for sustaining the amplitude of the cycle. A representative half cycle is shown in Figure 8 where the flame impingement, vortex impingement, and inter-element flow interactions can be identified. The half cycle starts off with the compression wave moving from right to left (1a) with unperturbed fuel injected from the two injectors (1b). Mixed fuel lies just downstream, left-over from a previous cycle, circulating near the wall and mixing between the injector elements. The heat release zone (1c) shows the majority of the heat release is occurring in the mixed fuel region. Just afterwards, a reacting portion of the left injector flame (shown in red) impinges against the left wall (2b). A local pressure increase is observed in this region and can be seen in pressure plot (2a).

As the cycle progresses, pressure continues to increase on the left side of the chamber (3a) and the original fuel vortex has grown larger (3b, circled in red). Additional vortices can also be seen between the two injector elements and appear to form in the strong pressure field. A decrease in heat release is seen between the injector elements (3c) as some of the fuel has burned away. In the last row (row 4) pressure has reached a maximum in the left side of the chamber and compression waves move upstream into the injector elements. The original fuel vortex (circled in 1b) has now impinged against the left wall but no large amount of heat release is seen in this zone. The largest heat release appears to be produced from the mixed methane gases downstream of the vortex and between the injector elements. This pattern appears commonly throughout the rest of the cycle. When a fuel vortex is initially shed from the lip, it produces only a small amount of heat release upon impingement with the wall. The majority of the heat release occurs a full cycle after the impinged vortex has had sufficient time to mix with the surrounding oxidizer.

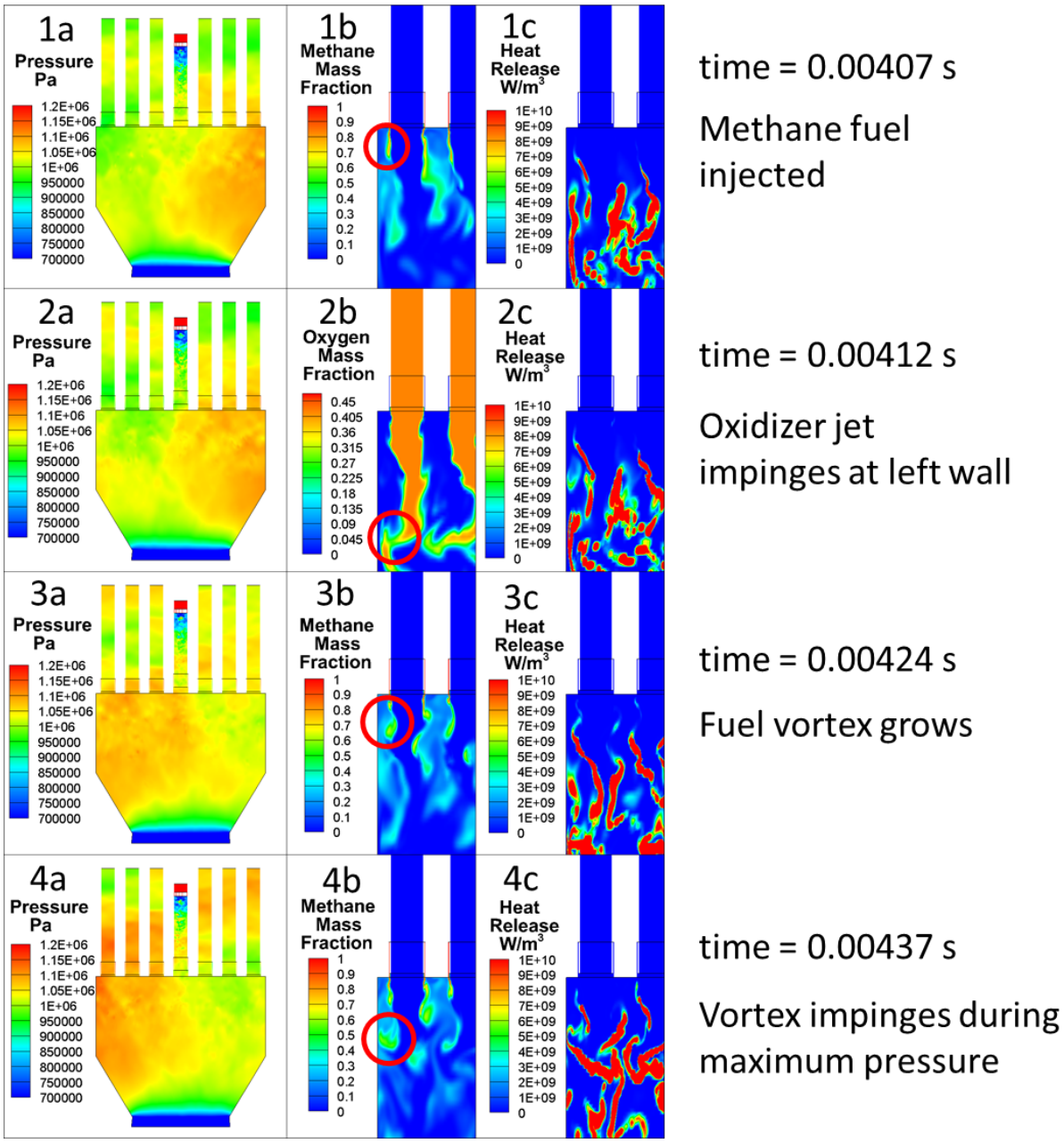


**Figure 8: A half cycle during the low amplitude instability stage is presented. Four points in time, corresponding to each row, are shown with pressure (a), fuel (b) and heat release (c) field plots.**

The low amplitude instability cycle presented here indicates that the heat release fluctuations between the injector elements and at the side-wall may not always couple with the primary transverse mode. This is further supported by looking at the spatial average of the heat release in both zones, plotted in Figure 9. The first zone encompasses the region where vortices impinge on the side-wall and the second spans the inter-element impingement zone. Both zones show the same initial low frequency response around 1 kHz as was seen in Figure 6. In the period of low amplitude instability (2.4 ms – 7.5 ms), there is evidence of activity around the 2 kHz and 4 kHz frequencies with a wider range of activity around the first acoustic mode.

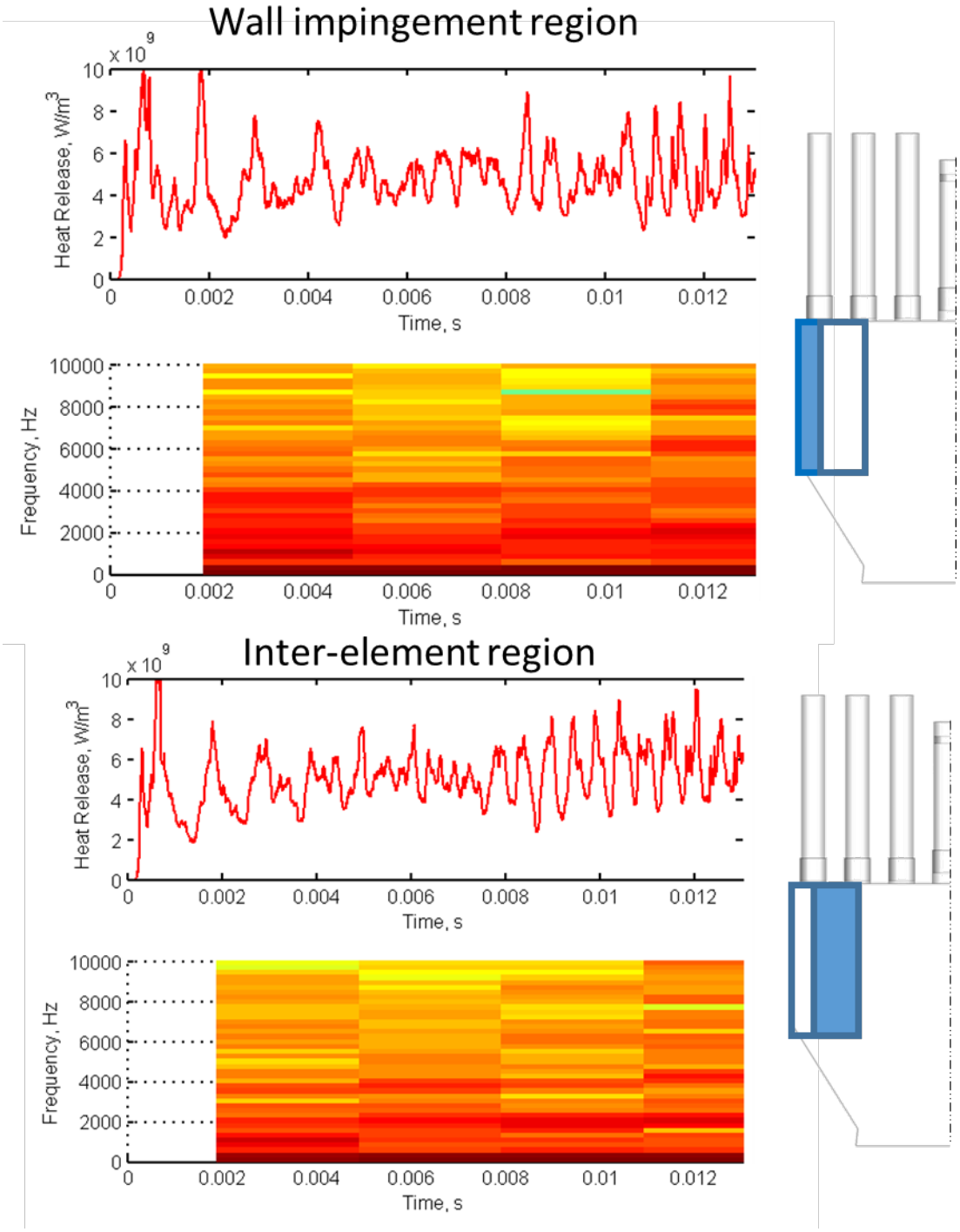


**Figure 9: Heat release zones showing the heat release signal capturing fluctuations near the wall boundary (top) and between injector elements (bottom).**

## D. High Amplitude Instability

The low amplitude instability stage transitions to the high amplitude instability stage around 7.5 ms and greater fluctuations are seen after this time with a stronger response occurring at the frequency of the first acoustic mode. This is especially evident in the inter-element region. As the instability amplitude grows there is evidence of strong fluctuations occurring at the first acoustic mode, while contributions from the higher harmonics are evident after 10 ms where the waveforms are clearly steep-fronted. The coupling of the heat release between the injector elements

with the acoustic modes may be responsible for driving the combustor to such strong amplitudes. Looking further at the flowfield during high instability amplitudes, a stronger production of heat release can be seen in regions of vortex impingement. This is shown in in Figure 10. In row one, the transverse wave begins to move to the left and vortices are collecting fuel and oxidizer from the injectors. As shown in 1b, fuel is being captured in vortices from injector 1 and between injectors 1 and 2. In row 2, the wave has travelled to the left of the chamber and reaches the peak pressure amplitude. At this point the vortices between injectors 1 and 2, as well as those between 2 and 3, impinge with each other while the vortex from injector 1 impinges against the wall. Comparing the heat release at the pressure peak (2c) versus a quarter cycle earlier (1c) shows that there is an increase in the combustion heat release between the injector elements in the region of vortex impingement. Like in the case of the low instability amplitude cycle, the majority of heat release near the left wall appears to originate from the mixed fuel downstream of the fuel vortex. The frequency of the heat release fluctuations in the inter-element and wall impingement regions match the frequency of the pressure fluctuations shown in Figure 5 and appear to show that the heat release fluctuations due to vortex impingement in the chamber are coupling with the acoustic mode. This in turn drives the combustor to stronger instability amplitudes. Throughout the high-amplitude stage, the instability continues to grow and the heat release appears further and further upstream due to the enhanced mixing between the injectors.

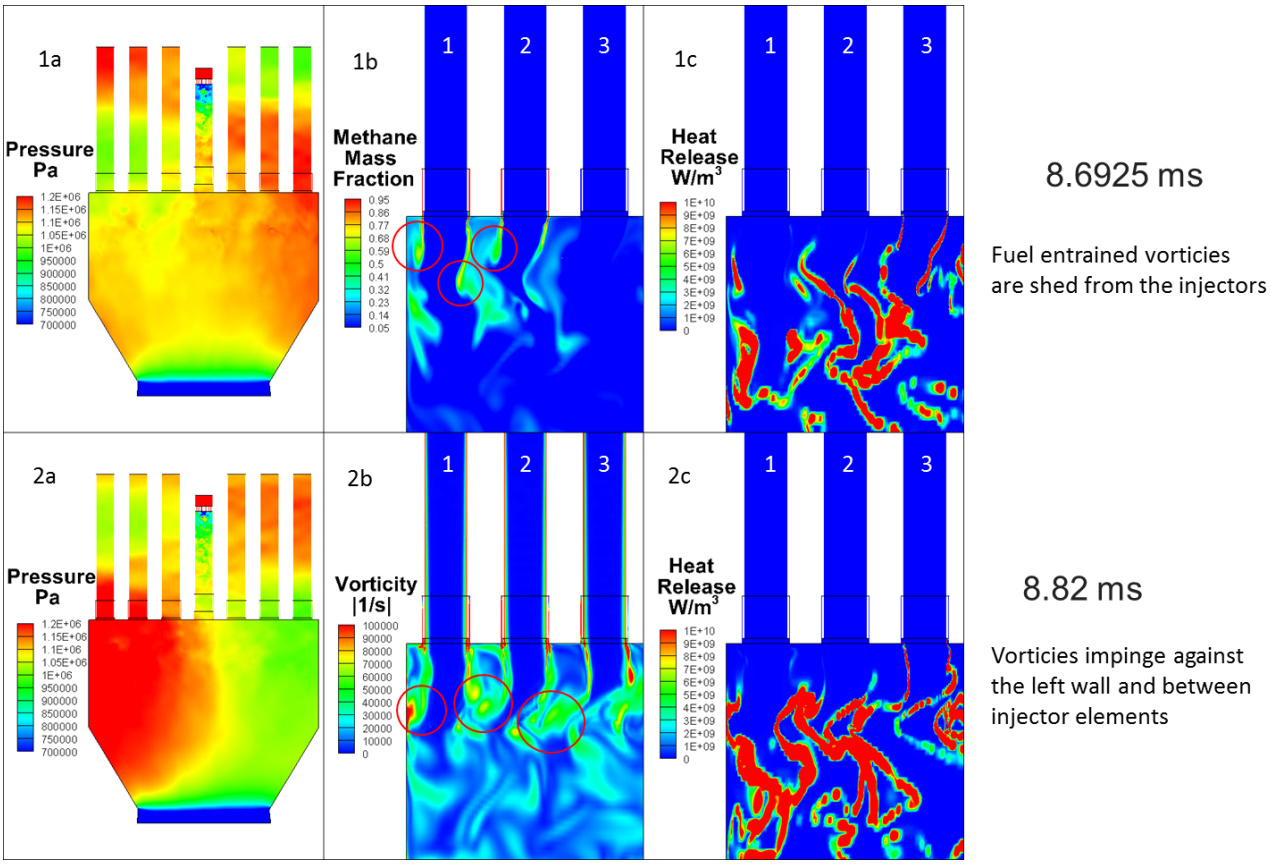


**Figure 10: During the high instability cycle fuel is captured in vortices as the transverse wave begins moving left (row 1) and at the pressure peak of the cycle (row 2) the vortices impinge causing a growth in heat release.**

## IV. Conclusions

A full geometry model of the seven-injector-element TIC has been developed using a one-step global reaction. Similar to the experiments, the computations predicted self-excited combustion instabilities. The results indicate that CFD can be used as a tool to explore transverse combustion instability mechanisms in multi-injector geometries. The simulation produced a range of oscillation amplitudes that allowed for the detailed examination of the salient thermoacoustic processes. Several insights were gained. It was learned that flame interaction with the walls and vortex interaction between injector elements may influence the instability amplitude. The instability first arose as the

side injector flames impinged against the converging chamber section with a strong pressure spike located towards one side of the chamber. A few characteristic differences between low amplitude and high amplitude instabilities were noted. First, during low amplitude oscillations, the flame interaction with the wall extended much further into the chamber, and into the converging section. The vortices also did not show a strong response to impingement between injector elements compared to the high amplitude instability stage.

The results provided good insight but are still limited in several ways. Unlike the experiment, a limit cycle was never reached and the high amplitude oscillations were not sustained. The reaction model applied is also very simple and likely leads to higher temperatures and more compact heat release modes than the experiment. The thermal boundary condition for the walls is adiabatic which does not allow for heat transfer to the metal chamber. Future work will focus on a comparison with the companion experiment, particularly in the flame zone, and the adjustment of the oxidizer injector lengths to explore their effects on combustion stability.

## Acknowledgments

The lead author was sponsored by a NASA Office of the Chief Technologist's Space Technology Research Fellowship. The companion experimental study was performed under contract FA9300-11-C-3006 to IN Space LLC, Mr. B.J. Austin Principal Investigator, and the Air Force Research Laboratory, Dr. Doug Talley Project Monitor. We would also like to thank Kevin Tucker and Matt Casiano of NASA Marshall Space Flight Center.

## References

1. Smith, D. A., Zukoski, E. E., "Combustion Instability Sustained by Unsteady Vortex Combustion," 21st JPC, AIAA-85-1248.
2. Poinsot, T. J., Trouve, A. C., Veynante, D. P., Candel, S. M., Esposito, E. J., "Vortex-driven acoustically coupled combustion instabilities," Journal of Fluid Mechanics, 1987, Vol. 177, pp. 265-292.
3. Ducruix, S., Schuller, T., Durox, D., Candel, S., "Combustion Dynamics and Instabilities: Elementary Coupling and Driving Mechanisms," Journal of Propulsion and Power, Vol. 19, No. 5, September – October 2003.
4. Menon, S, Jou, W. H., "Large-Eddy Simulations of Combustion Instability in an Axysymmetric Ramjet Combustor," 28th ASM, AIAA-90-0267.
5. Veynante, D., Pointsot, T., "Large eddy simulation of combustion instabilities in turbulent premixed burners," Center for Turbulence Research, Annual Research Briefs, 1997.
6. Brookes, S. J., Cant, R. S, Dupere, I. D. J., Dowling, A. P., "Combutational Modeling of Self-Excited Combustion Instabilities, ASME, Vol. 123, April 2001.
7. Selle, L., Benoit, L., Poinsot, T., Nicoud, F., Krebs, W., "Joint use of compressible large-eddy simulation and Helmholtz solvers for the analysis of rotating modes in an industrial swirled burner," Combustion and Flame, Vol 145, 2006, pp. 194 – 205.
8. Smith, R. J., Computational Investigations of High Frequency Acoustics and Instabilities in a Single-Element Rocket Combustor, PhD Dissertation, Purdue University, West Lafayette, IN, August 2010.
9. Xia, G., Harvazinski, M., Anderson, W., Merkle, C. L., "Investigation of Modeling and Physical Parameters on Instability Prediction in a Model Rocket Combustor," 47th JPC, AIAA 2011-6030.
10. Harvazinski, M. E., Modeling Self-Excited Combustion Instabilities Using A Combination of Two- and Three-Dimensional Simulations, PhD Dissertation, Purdue University, West Lafayette, IN, May 2012.
11. Garby, R., Selle, L., Poinsot, T., "Large-Eddy Simulation of combustion instabilities in a variable-length combustor," C. R. Mecanique, Vol. 341, 2013, pp. 220-229.
12. Shipley, K., Morgan C., Anderson, W. E., Harvazinski M. E., Sankaran, V., "Computational and Experimental Investigation of Transverse Combustion Instabilities," 49th JPC, AIAA 2013-3992.
13. Smith, R., Xia, G., Anderson, W., Merkle, C. L., "Extraction of Combustion Instability Mechanisms form Detailed Computational Simulations," 48th ASM, AIAA 2010-1152.
14. Smith, R., Xia, G., Anderson, W., Merkle, C. L., "Computational Studies of the Effects of Oxidizer Injector Length on Combustion Instability," Combustion Theory and Modeling, 2011, DOI:10.1080/13647830.2011.631031
15. Harvazinski, M. E., Anderson, W., Merkle, C. L., "Analysis of Self-Excited Combustion Instabilities Using Two- and Three-Dimensional Simulations," Journal of Propulsion and Power, Vol. 29, No. 2, March-April 2013.
16. Harvazinski, M. E., Huang, C., Sankaran, V., Feldman, T., Anderson, W., Merkle, C. L., Talley, D. G., "Combustion Instability Mechanisms in a Pressure-coupled Gas-gas Coaxial Rocket Injector," 49th JPC,

AIAA 2013-3990.
17. Hermeth, S., Staffelbach, G., Gicquel, L. Y. M., Poinsot, T., “LES evaluation of the effects of equivalence ratio fluctuations on the dynamic flame response in a real Gas Turbine Combustion Chamber,” Proceedings of the Combustion Institute, Vol. 34, no. 2, pp. 3165 – 3173, ISSN 1540-7489, 2013.
18. Krediet, Prediction of Limit Cycle Pressure Oscillations in Gas Turbine Combustion Systems Using the Flame Describing Function, PhD Dissertation, University of Twente, June 2012.
19. Morgan, C. J., Pomeroy, B. R., Anderson, W. E., “Implementation of a 2D Chamber to Study the Response of a Gas-Gas Injector to Transverse Instability,” JANNAF, April 2013.
20. Li, D., Xia, G., Sankaran, V., and Merkle, C., “Computational Framework for Complex Fluids Applications," 3rd International Conference on Computational Fluid Dynamics, Toronto, Canada, July 2004.
21. Xia, G., Sankaran, V., Li, D., and Merkle, C., “Modeling of Turbulent Mixing Layer Dynamics in Ultra-High Pressure Flows," 36th AIAA Fluid Dynamics Conference and Exhibit, San Francisco, CA, June 2006, AIAA Paper 2006-3729.
22. Lian, C., Xia, G., and Merkle, C., “Impact of Source Terms on Reliability of CFD Algorithms," The 19th AIAA Computational Fluid Dynamics, San Antonio, TX, June 2009.
23. Lian, C., Xia, G., and Merkle, C., “Solution-Limited Time Stepping to Enhance Reliablity in CFD Applications," Journal of Computational Physics, Vol. 228, 2009, pp. 4836-4857
24. Spalart, P., Jou, W., Strelets, M., and Allmaras, S., “Comments on the feasibility of LES for wings on a hybrid RANS-LES approach,” 1st U.S. Air Force Office of Scientific Research Office Conference on DNS/LES, Columbus, OH, August 1997, pp. 137-148.
25. Travin, A., Shur, M., and Splart, P., “Physical and numerical upgrades in the detached-eddy simulation of complex turbulent flows,” 412 EUROMECH Colloquium on LES of Complex Transitional and Turbulence Flows, Munich, October 2000.
26. Wilcox, D., Turbulence Modeling for CFD, DCW Industries, 1998.
27. Wilcox, D., “Formulation of the k-ω turbulence model revisited,” 45th AIAA Aerospace Sciences Meeting and Exhibit, AIAA, Reno, NV, January 2007.
28. McBride, B. J., and Gordon, S., Computer Program for Calculating and Fitting Thermodynamic Functions, NASA RP 1271, 1992.
29. Westbrook, C., Dryer, F., “Simplified Reaction Mechanisms for the Oxidation of Hydrocarbon Fuels in Flames,” Combustion and Science Technology, 1981 Vol. 27, pp. 31 – 43.